

## Supplementary material

**Table S1.** Biogenic CO<sub>2</sub> fluxes used for estimating the XCO<sub>2</sub> uncertainty resulting from the uncertainty in the biogenic flux.

Data	Temporal resolution	Spatial resolution	Flux
VISITc*	Hourly	~0.31°	Net ecosystem exchange
SiB4	Hourly	0.5°	Net ecosystem exchange
CarbonTracker 2019B	3-hourly	1°	Optimized biogenic and oceanic fluxes
BEAMS	Monthly	30 arcsec	Net ecosystem exchange

\*Downscaled by green vegetation fraction data

**Table S2.** Annual CO<sub>2</sub> emissions in fiscal year 2015 reported by four administrative divisions located in southern Kanto.

Division	Annual CO <sub>2</sub> emission (Mt-CO <sub>2</sub> yr <sup>-1</sup> )	Reference
Tokyo	60.33	<a href="https://www.kankyo.metro.tokyo.lg.jp/en/climate/index.files/Tokyo_GHG_2019.pdf">https://www.kankyo.metro.tokyo.lg.jp/en/climate/index.files/Tokyo_GHG_2019.pdf</a>
Chiba	78.497	<a href="https://www.pref.chiba.lg.jp/shigen/chikyuukankyou/documents/2017haisyutsuryou.pdf">https://www.pref.chiba.lg.jp/shigen/chikyuukankyou/documents/2017haisyutsuryou.pdf</a>
Kanagawa	70.24	<a href="https://www.pref.kanagawa.jp/documents/9881/g hg_siryō.pdf">https://www.pref.kanagawa.jp/documents/9881/g hg_siryō.pdf</a>
Saitama	41.541	<a href="https://www.pref.saitama.lg.jp/documents/25672/r4zentaihoukokusyo.pdf">https://www.pref.saitama.lg.jp/documents/25672/r4zentaihoukokusyo.pdf</a>

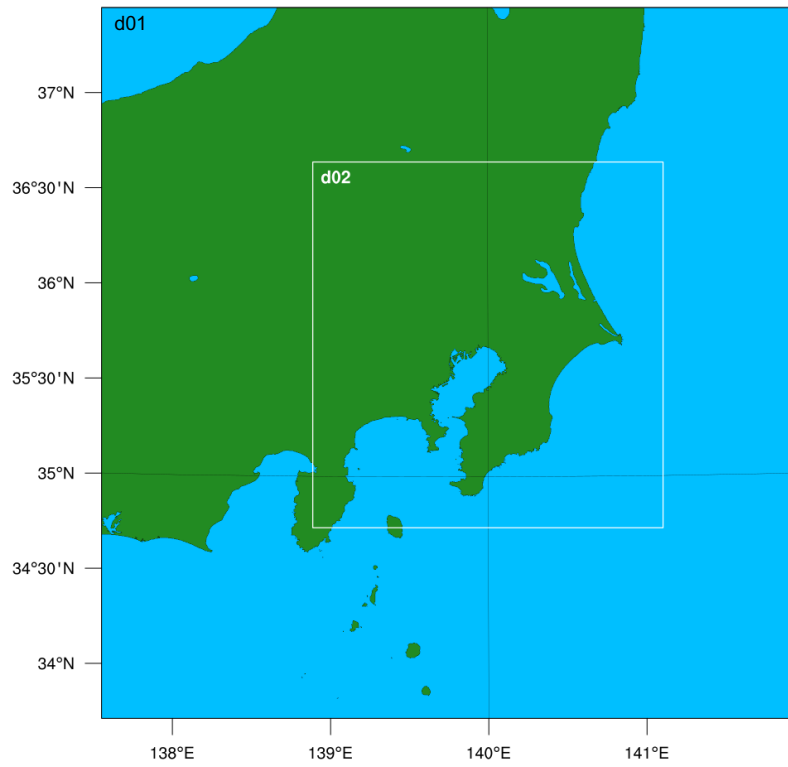


**Figure S1.** Domain configuration for the WRF simulation.

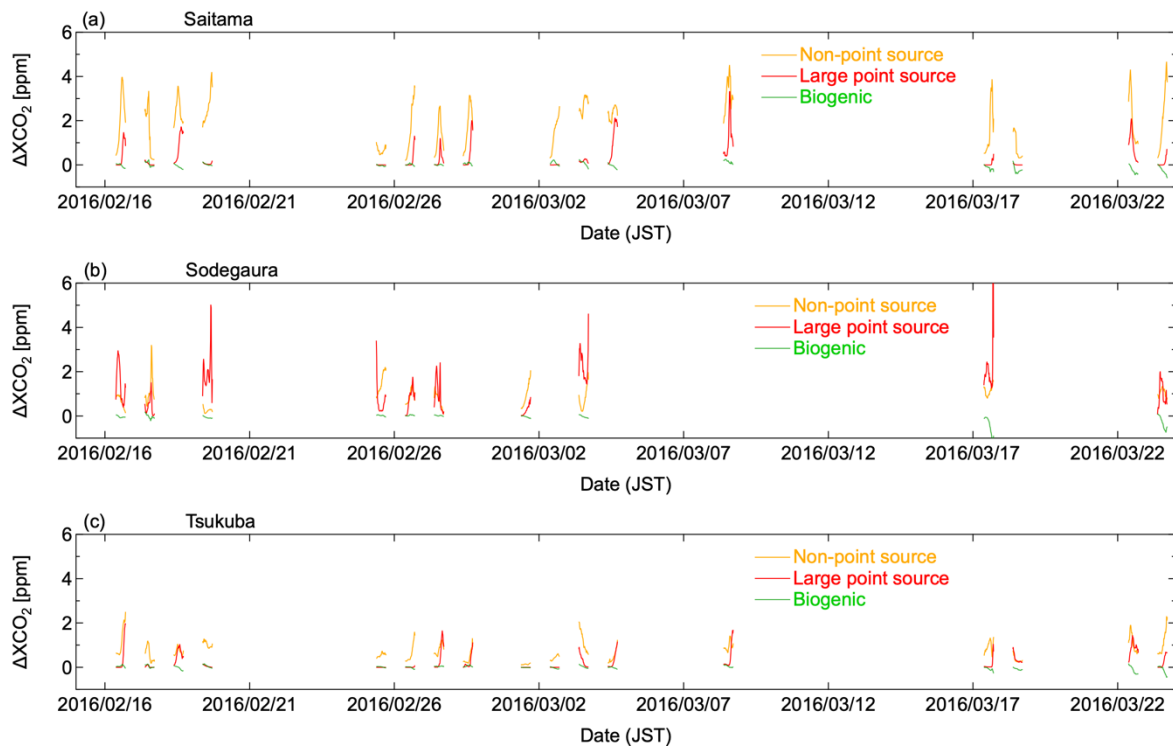


**Figure S2.**  $\Delta XCO_2$  values at (a) Saitama, (b) Sodegaura, and (c) Tsukuba simulated separately from nonpoint sources, large point sources, and biogenic fluxes.

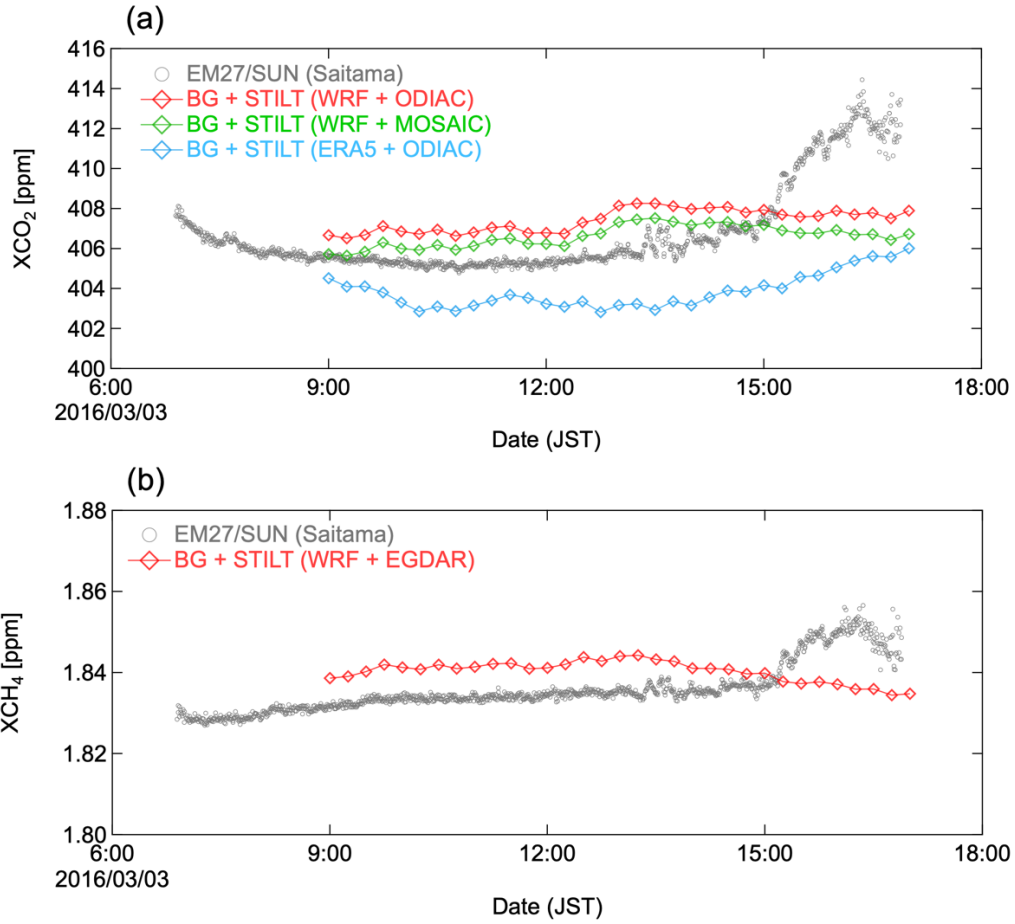


**Figure S3.** Comparison of (a) XCO<sub>2</sub> and (b) XCH<sub>4</sub> observations at Saitama on 3 March 2016 with STILT simulation results. The XCO<sub>2</sub> simulations were performed using three different combinations of meteorological fields and emission data, whereas the XCH<sub>4</sub> simulation was performed using the WRF model and EDGAR data.

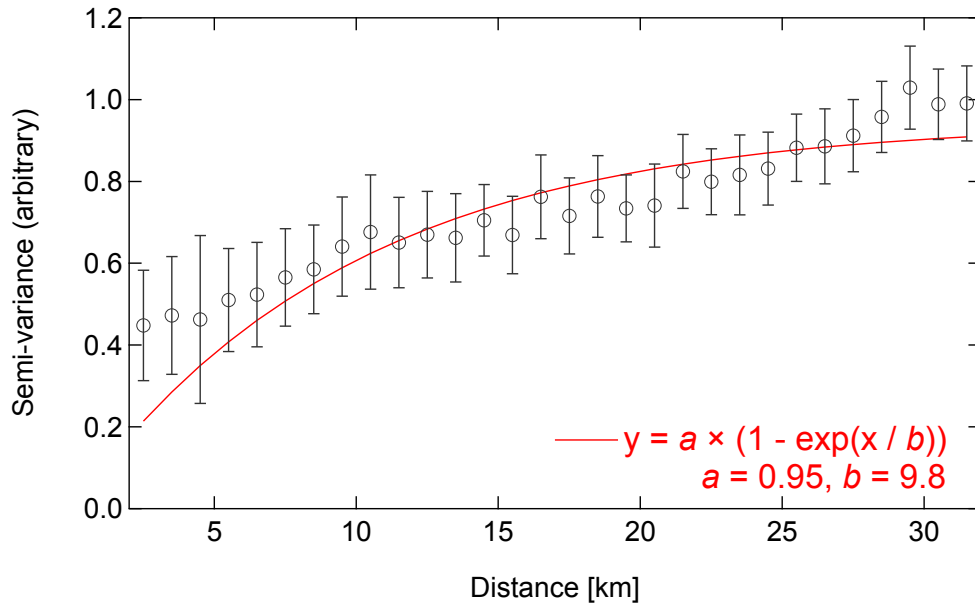


**Figure S4.** Semi-variogram calculated from the differences in nonpoint source elements between the ODIAC and MOSAIC emission data with both aggregated into a spatial resolution of  $0.025^\circ \times 0.025^\circ$ . The error bars indicate the standard error of each 1 km bin. The red line is the fitted curve with coefficients  $a$  and  $b$ , where coefficient  $b$  corresponds to the spatial correlation length.

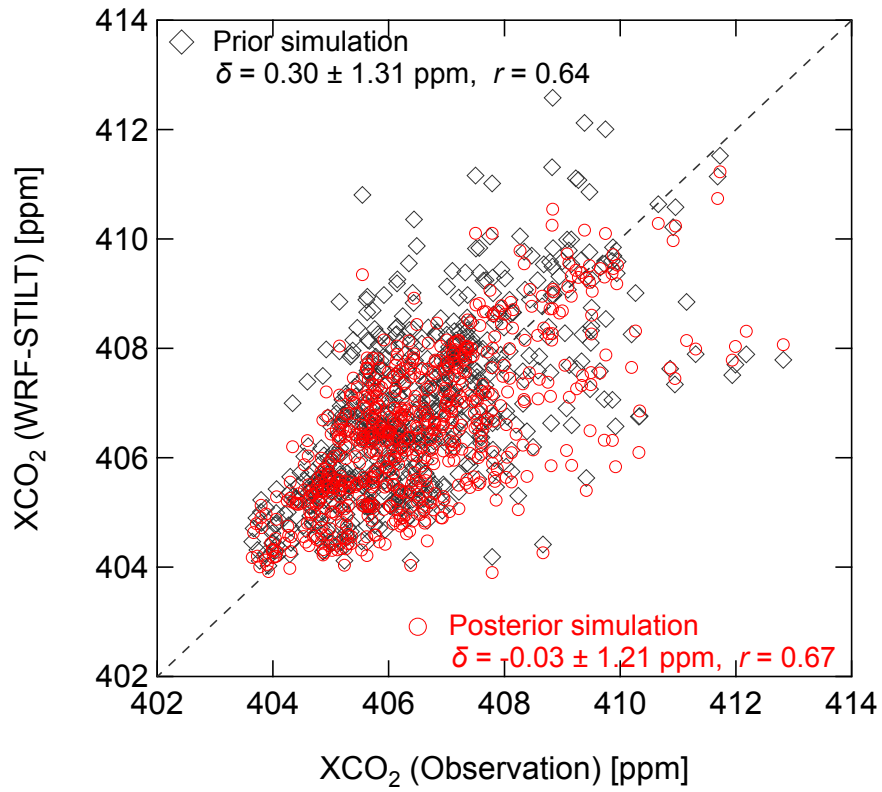


**Figure S5.** Scatter plot of observed XCO<sub>2</sub> values and values simulated from the prior (black) and posterior (red) emission fluxes. The mean difference between the simulations and observations (simulation minus observation) with the standard deviation ( $\pm 1\sigma$ ) is denoted as  $\delta$ , and  $r$  is the correlation coefficient.

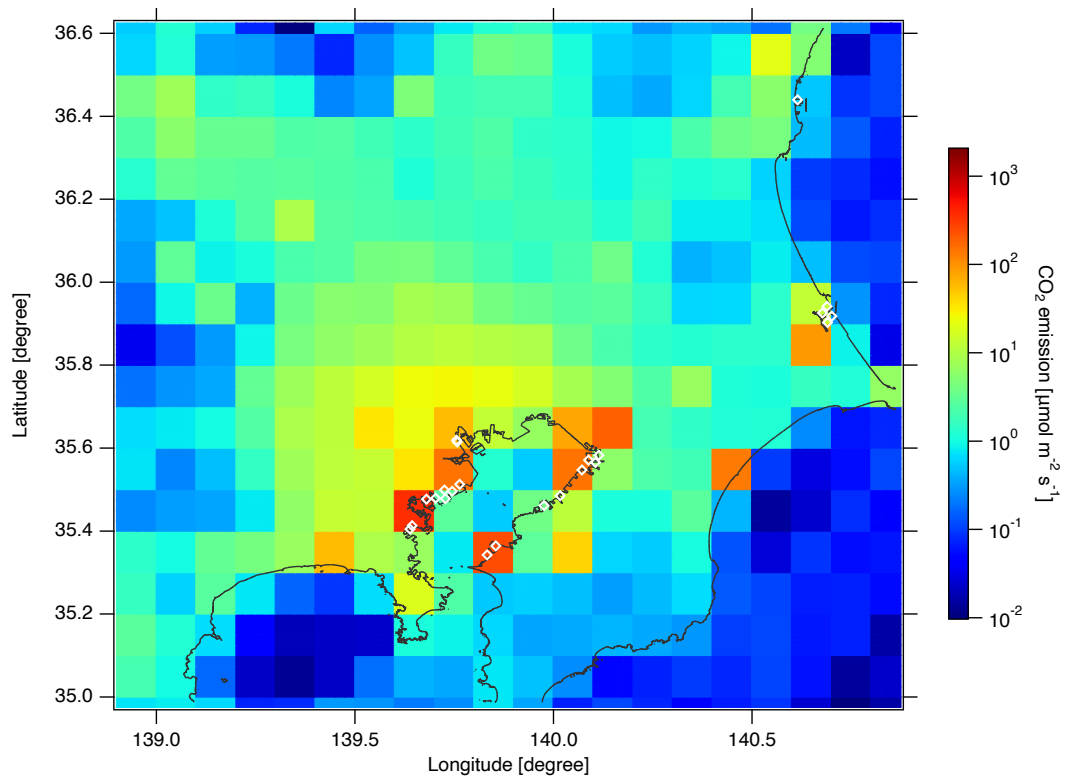


**Figure S6.** EDGAR version 6 CO<sub>2</sub> emission fluxes in the TMA in 2016. White diamonds indicate the locations of the large point sources considered in this study.



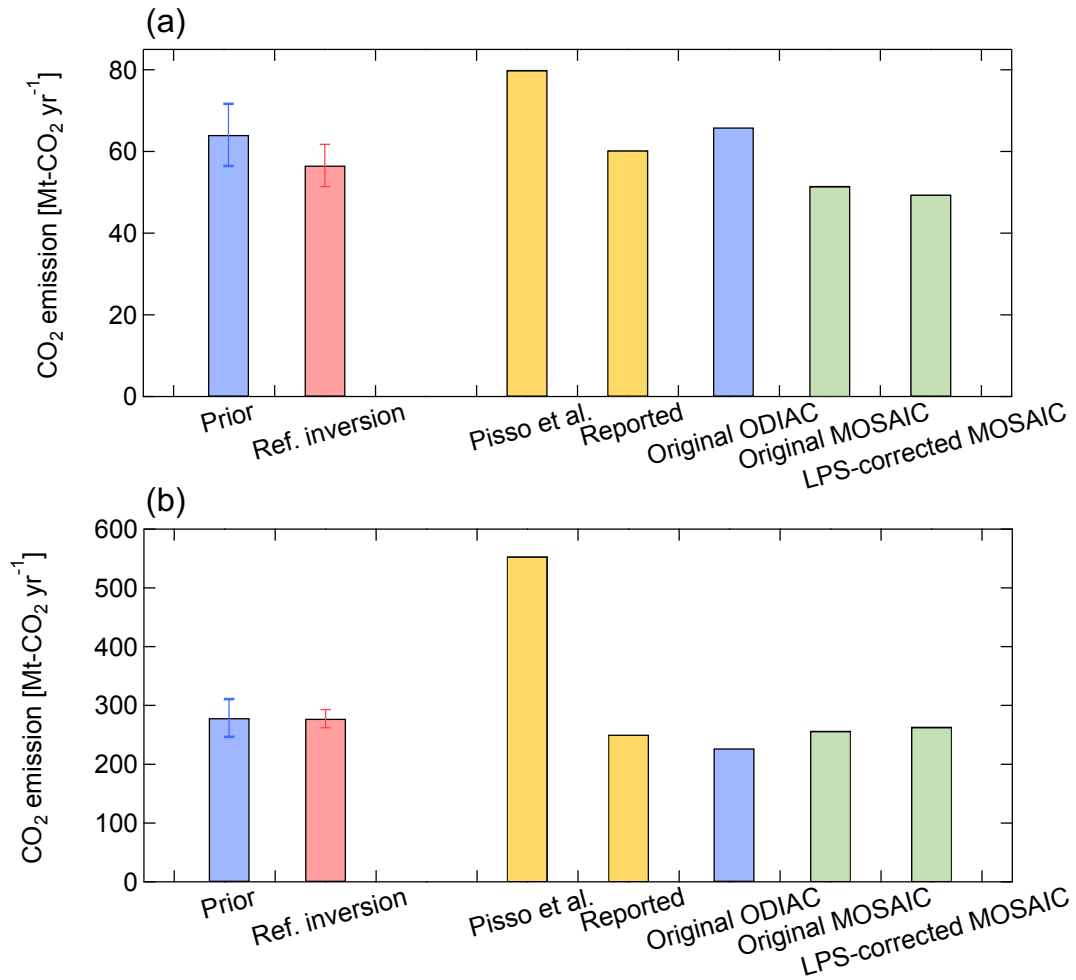


**Figure S7.** CO<sub>2</sub> emissions in (a) the Tokyo Metropolis and (b) southern Kanto (Tokyo Metropolis and Kanagawa, Saitama, and Chiba Prefectures) calculated from the posterior fluxes of the reference inversion (red), the ODIAC data (blue), and the MOSAIC data (green). The error bars for the prior and posterior estimates indicate uncertainties at the 95 % confidence level. For the ODIAC and MOSAIC data, both original and LPS-corrected total emissions are shown. Also shown are the CO<sub>2</sub> emissions for the corresponding domains extracted from Pissó et al. (2019) and the values reported by the administrative divisions (yellow).